ResearchGate

See discussions, stats, and author profiles for this publication at: https://www.researchgate.net/publication/286451131

Assessing the Impact of Urbanization on Urban Thermal Environment: A Case Study of Bangkok Metropolitan

Article · August 2012

CITATIONS
80

READS
2,467

3 authors:

Manat Srivanit
Thammasat University
61 PUBLICATIONS **667** CITATIONS
SEE PROFILE

Kazunori Hokao
Saga University
116 PUBLICATIONS **2,645** CITATIONS
SEE PROFILE

Vivarad Phonekeo
Asian Institute of Technology
15 PUBLICATIONS **123** CITATIONS
SEE PROFILE

Some of the authors of this publication are also working on these related projects:

Stochastic Urban Growth Model View project

A Study of Connectivity between the Sub-Urban Railway Stations and Surrounding Communities around Thammasat University (TU) View project

All content following this page was uploaded by Manat Srivanit on 11 December 2015.

The user has requested enhancement of the downloaded file.

Assessing the Impact of Urbanization on Urban Thermal Environment: A Case Study of Bangkok Metropolitan

Manat SRIVANIT
Doctor Student
Social System Management Laboratory
Japanese Government (Monbukakusho) Scholarship 2010
Postgraduate Special Joint Program (PSJP) for Students in Environmental Earth Sciences and Technology, Saga University, Japan

Kazunori Hokao
Graduate School of Science and Engineering, Saga University, Saga 840-8502, JAPAN

Vivarad Phonekeo
Geoinformatics Center, Asian Institute of Technology, Pathumthani 12120, Thailand

Abstract

The Bangkok metropolitan area (BMA) is one of the regions experiencing rapid urbanization that has resulted in remarkable the urban thermal environment problems, which will be sure to influence the regional climate, environment, and socio-economic development. In this study, LANDSAT Thematic Mapper (TM) imagery from 1994, 2000 and 2009, were utilized to assess urban area thermal characteristics by investigating the relationships between the land surface temperature (LST) and the Normalized Difference Vegetation Index (NDVI). It was found that average surface temperature (Mean±S.D.) in the BMA was about 26.01±5.89˚C in 1994, but this difference jumped to 37.76±2.84˚C in 2000 and further to 39.79±2.91˚C in 2009, respectively. This could lead to an intensified urban thermal effect in the urban areas. Overall, remote sensing technology was effective approaches for aiming at environment monitoring and analyzing urban growth patterns and evaluating their impacts on urban climates.

Keywords*:* Urban heat island (UHI); Land surface temperature (LST); Normalized Difference Vegetation Index (NDVI); Landsat Thematic Mapper (TM)

1. Introduction

Urbanization transforms the natural landscape to anthropogenic urban land and changes surface physical characteristics. Of these effects, one of the most important is surface temperature variation. Land surface temperature is very important to the study of urban climates (Voogt&Oke, 2003). It modifies the air temperature of the atmospheric boundary layer and is a key component in the surface energy balance. Change in urban land surface temperature can have significant effects on local weather and climate (Kalnay&Cai, 2003; Landsberg, 1981). By covering the landscape with buildings, roads, parking lots, and other paved surfaces, urban areas usually have higher solar radiation absorption and a greater thermal conductivity and capacity for releasing heat stored during the day at night. This procedure generally leads to a modified climate that is warmer than the surrounding rural areas and is referred to as an urban heat island (UHI) (Voogt&Oke, 2003). The higher temperatures in urban heat islands increase air conditioning demands, raise pollution levels, and may modify precipitation patterns. As a result, the magnitude and pattern of UHI effects have been major concerns of many urban climatology studies.

UHI have long been studied by ground-based observations taken from fixed thermometer networks or by traverses with thermometers mounted on vehicles. With the advent of thermal remote sensing technology, remote observation of UHI became possible using satellite and aircraft platforms and has provided new avenues for the observation of UHI, to perform land cover classifications and as input for models of urban surface atmosphere exchange. Voogt and Oke (2003) suggested three major applications of thermal remote sensing to the study of urban climates. Two of them focus on examining relations either between spatial structure of urban thermal patterns and urban surface characteristics or between atmospheric and surface heat islands; the third is centered on studying urban surface energy balances by coupling urban climate models with remotely sensed data. Our study addresses the first application area.

Rao (1972) was the first to demonstrate that urban areas could be identified from the analyses of thermal infrared data acquired by a satellite. Gallo et al. (1995) reviewed and represented a satellite perspective on the assessment of UHI. Studies on the UHI phenomenon using satellite derived land surface temperature (LST) measurements have been conducted primarily using NOAA AVHRR data (Gallo & Owen, 1998a,b; Streutker, 2002) for regional-scale urban temperature mapping. Recently, Landsat Thermatic Mapper (TM) and Enhanced Thermatic Mapper Plus (ETM+) thermal infrared (TIR) data with 120 m and 60 m spatial resolutions, respectively, have also been utilized for local-scale studies of UHI (Chen,Wang, & Li, 2002; Weng, 2001). Research on LST showed that the partitioning of sensible and latent heat fluxes and thus surface radiant temperature response was a function of varying surface soil water content and vegetation cover (Owen et al., 1998). This finding encourages research on the relationship between LST and vegetation abundance (e.g. Gallo & Owen, 1998a,b; Weng, 2001; Weng et al., 2004).

UHI intensity is related to patterns of land use/cover changes (LUCC), e.g. the composition of vegetation, water and built-up and their changes. Hawkins et al. (2004) studied the effect of rural variability in calculating the urban heat island effect. Qualitative studies on the relationship between land use/cover pattern (LUCP) and LST will help us in land use planning. It is known that various vegetation indices obtained from remote sensing images can be used in the assessment of vegetation cover qualitatively and quantitatively (Tian & Xiangjun, 1998). Relationships between various vegetation indices and percent vegetation cover have been established by using regression analysis (Purevdorj, Tateishi, Ishiyama, & Honda, 1998), such as Ratio Vegetation Index (RVI), Normalized Difference Vegetation Index (NDVI), Difference Vegetation Index (DVI) and Perpendicular Vegetation Index (PVI). The NDVI has been used for the estimation of vegetation productivity and rainfall in semiarid areas (Chen et al., 2004; Wang et al., 2004). It is possible that the utilization of LST and NDVI could represent land-cover types quantitatively so that the relationships between NDVI and temperature can be established in UHI studies.

The purpose of our study is to examine the changes in land use/cover pattern in a rapidly changing area of the Bangkok Metropolitan Area (BMA) in relation to urbanization since the 1994 and then to investigate the impact of such changes on the intensity and spatial pattern of the UHI effect in BMA. We used NDVI indices to extract land use/cover information from remote sensing images of different time periods and then analyzed the surface temperature retrieved from the thermal infrared band. The specific objectives of this research are: (1) to derive brightness temperature from the Landsat TM thermal band for the period 1994, 2000 and 2009; (2) to examine the spatial pattern of the land use/cover index values and their changes over the study period; (3) to investigate the relationship between brightness temperature and land use/ cover pattern (LUCP) in the BMA ; and (4) to quantitatively study the relationship between the intensity of UHI and LUCP and how it has changed over time.

2.The Study Area

Bangkok is the capital of Thailand and is among the larger cities in Asia, with an estimated unofficial population well in excess of 10 million people. As an economic magnet, Bangkok's population is continually increasing through in-migration from the Thai countryside. This rapid rise in population, capital investment, factories and employees in Bangkok city have caused the community numbers to increase leading to the development of road networks, real estate developments, land value and advanced technologies which has resulted in expansion of the city to the surrounding areas (Fig.1). This rapid urbanization has led to several environmental problems such as air pollution, water pollution, land subsidence as well as the effect of urban heat island.

Furthermore, as cities continue to grow in both population and physical size, these urban–rural differences in temperature also increase as reported by long-term temperature records. Boonjawat et al. (2000) found an increase of 1.23 ˚C in lowest air temperature in the UHI of Bangkok for the last 50 years and the peak temperature of metropolitan such as Bangkok can be higher than the surroundings by 3.5 ˚C is detected during clear and clam night in dry season. Increased temperatures due to the UHI effect may increase water consumption and energy use in urban areas and lead to alterations to biotic communities (White, Nemani, Thornton, &Running,2002). Kiattiporn et al. (2008) found an increase in 1˚C of the temperature will result in an increase of 6.79% electricity consumption in BMA. Excess heat may also affect the comfort of urban dwellers and lead to greater health risks (Poumadere, Mays, LeMer,&Blong,2005).

In addition, higher temperatures in urban areas increase the production of ground level ozone which has direct consequences for human health (Akbari, Rosenfeld, Taha,&Gartland, 1996; Akbarietal., 2001). It is, therefore, analyzing patterns of UHI in BMA and its relationship with urban surface characteristics is significant to understand in order to lessen the ever worsening urban climate problem in the region.

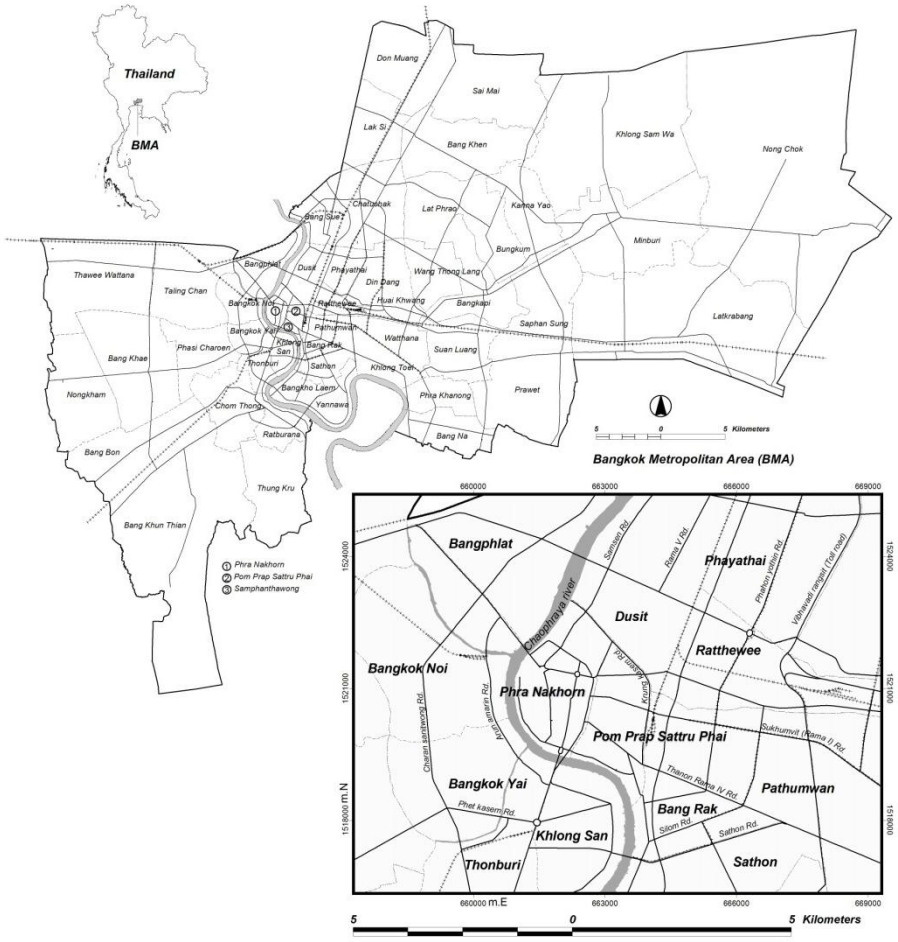

Fig.1. Location of the Bangkok Metropolitan Area (BMA), Thailand

3. Methods

3.1. Image pre-processing

Landsat data from two different years were obtained. Landsat thematic mapper (TM) images acquired on March 5th, 1994, February 18th, 2000 and April 25th, 2009 were geo-referenced to a common UTM coordinate system based on the rectified high resolution QuickBird image, aerial photograph and the 1:50,000 scale topographic maps. Using the radiometric correction method of Schroeder et al. (2006), the original digital numbers of bands 1–5 and 7 images were converted to at-satellite radiance, at satellite reflectance, and further converted to surface reflectance. While bands 1 through 5 and band 7 are at a spatial resolution of 30 m., the thermal infrared band (band 6) comes at an original spatial resolution of 120 m. for Landsat 5 TM images.

3.2. Image classification

In order to examine the impacts of human activities on regional scale, a land cover classification is necessary for detection of LULC during the rapid urbanization since the 1994s. In this study, the Landsat Thematic Mapper (TM) data acquired on 1994, 2000 and 2009 were used. The categories include: (1) urban or built-up area, (2) vegetated areas (including the forest, farmland, and shrub), (3) water bodies (mainly including rivers, creeks, ponds, and lakes) and (4) Other (bare land).

This study requires the detection of fine changes in surface reflectances, radiometric correction became necessary. A supervised signature extraction with the maximum likelihood algorithm was employed to classify the Landsat images. Both statistical and graphical analyses of feature selection were conducted, and bands 2 (green), 3 (red), and 4 (near infrared) were found to be most effective in discriminating each categories and thus used for classification. Training site data were collected by means of on-screen selection of polygonal training data method, was chosen for each image to ensure that all spectral classes constituting each land use and land cover category were adequately represented in the training statistics. The accuracy of the three classified maps was checked with a stratified random sampling method, by which 50 samples were selected for each land use and land cover category. The reference data was collected from field survey or from existing land use and cover maps that have been field-checked. Largescale aerial photos were also employed as reference data in accuracy assessment when necessary.

3.3. Derivation of LST and NDVI from Landsat TM imageries

3.3.1. Derivation of land surface temperature

LST is the radiative skin temperature of the land surface, which plays an important role in the physics of the land surface through the process of energy and water exchanges with the atmosphere. The derivation of LST from satellite thermal data requires several procedures: sensor radiometric calibrations, atmospheric and surface emissivity corrections, characterization of spatial variability in land-cover, etc. As the near-surface atmospheric water vapour content varies over time due to seasonality and inter-annual variability of the atmospheric conditions, it is inappropriate to directly compare temperature values represented by the LST between multiple periods. Therefore the focus here is on the UHI intensity and its spatial patterns across the study region. UHI intensity is estimated as the difference between the peak temperatures (LST) of the urban area and the background non-urban temperatures (Chen et al., 2006). This UHI effect can be determined for the individual thermal images and then compared between two or more periods. However, before we compute UHI effect, we must first derive the LST based on methods for ETM+ images.

As described above the Landsat TM thermal infrared band (10.4–12.5 μm) data were used to derive the LST. Yuan and Bauer (2005) proposed a method of deriving LST in three steps: Firstly, the digital numbers (DNs) of band 6 are converted to radiation luminance or top-of-atmospheric (TOA) radiance (L_λ , mW/(cm^2 sr·μm) using (Eq. [1]) (Chander & Markham, 2003):

$$L_\lambda = \frac{(L_{max} - L_{\min})}{QCAL_{max} - QCAL_{\min}} \times (DN - QCAL_{\min}) + L_{\min} \qquad [1]$$

Where *DN* is the pixel digital number for band 6, $QCAL_{\max}$ = 255 is Maximum quantized calibrated pixel value corresponding to $L_{\max}$, $QCAL_{\min}$ = 0 is Minimum quantized calibrated pixel value corresponding to $L_{\min}$, $L_{\max}$ = 17.04 (mW/cm^{2}sr·μm) is spectral at-sensor radiance that is scaled to $QCAL_{\max}$ and $L_{\min}$ = 0 (mW/cm^{2}sr·μm) is spectral at-sensor radiance that is scaled to $QCAL_{\min}$.

Secondly, the radiance was converted to surface temperature using the Landsat specific estimate of the Planck curve (Eq. [2]) (Chander & Markham, 2003):

$$T_k = \frac{K2}{In\left(\frac{K1}{L_\lambda} + 1\right)} \qquad [2]$$

Where T_k is the temperature in Kelvin (K), $K1$ is the prelaunch calibration of constant 1 in unit of W/(m^2 sr·μm) and $K2$ is the prelaunch calibration constant 2 in Kelvin. For Landsat TM, $K1$ is about 607.76 W/(m^2 sr·μm) and $K2$ is about 1260.56 W/(m^2 sr·μm) with atmospheric correction (Barsi et al., 2003). The final apparent surface temperature on Celsius (˚C) can be calculated the following equation:

$$T_c = T_k - 273.15 \qquad [3]$$

Where T_c is the temperature in Celsius (˚C), T_k is the temperature in Kelvin (K).

3.3.2. Derivation of normalized difference vegetation index

Normalized difference vegetation index (NDVI) may be used as an indicator of biomass and greenness (Myneni et al., 2001; Chen and Brutsaert, 1998). When standardized, it may also be used as a method for comparing vegetation greenness between satellite images (Gillies et al., 1997; Weng and Lo, 2001). The index value is sensitive to the presence of vegetation on the Earth's land surface, and is also highly correlated with climatic variables, such as precipitation (Schmidt and Karnieli, 2000). In this study, NDVI were used to examine the relationship between LST and greenness. NDVI were calculated as the ratio between measured reflectance in the red and near infrared (NIR) spectral bands of the images using the following formula:

$$NDVI = \frac{R_{NIR} - R_{red}}{R_{NIR} + R_{red}} \qquad [4]$$

Where R_{NIR} and R_{red} are spectral reflectance in Landsat TM red (band3) and near-infrared (band4) bands. Calculations of NDVI for a given pixel always result in a number that ranges from minus one (-1) to plus one (+1); however, no green leaves gives a value close to zero. A zero means no vegetation and close to +1 (0.8 - 0.9) indicates the highest possible density of green leaves.

These indices could be used to classify different land use/cover types (e.g., vegetation, water, built-up), Index value ranges for these land-cover types are not constant, which will have little changes in different regions or in different conditions of atmosphere and precipitation. Sometimes, several indices are integrated to differentiate different land use/cover types.

4. Result and Discussion

4.1. Land use/cover patterns and changes in BMA

In Bangkok, the expansion of urban land use is characterized by unplanned, sprawl and ineffectively regulated. Such a rapid growth in terms of population and economic activities took place in horizontal manner to the provinces surrounding Bangkok, causing degradation of agricultural areas. Agricultural land was converted to urban uses as Bangkok expanded along three major transport corridors to the southwest, southeast and north of the city. Three dates of fraction images were classified into three thematic maps. Figs. 2 show the classified maps. Conversion of other LULC types into urban/built-up land was further illustrated in Table 1 breaks down LULC changes. In the Bangkok Metropolitan Area (BMA) (1,576.10 sq. km.), urban/built-up land increased by almost three times from 1994 to 2009, which grew from 15% in 1994, to 33% in 2000, leveling out in 2009 to 42% of the total area (Fig.2). In contrast, a pronounced decrease in the vegetated area was discovered from 1994 (72%), 2000 (49%) and 2009 (40%), respectively. This decrease was also evident between 1994 and 2000, when vegetated area was further shrunk by 353.57 sq.km. or about 22% of the total area, was converted to other land use.

Most of the urban expansion resulted from the conversion of agricultural land, most of which involved land under rice cultivation. Urbanization negatively impacts the environment mainly by the production of pollution, the modification of the physical and chemical properties of the atmosphere. It is well-known that the progressive replacement of natural surfaces by built surfaces, through urbanization, constitutes the main cause of UHI formation. Natural surfaces are often composed of vegetation and moisture-trapping soils. Therefore, they utilize a relatively large proportion of the absorbed radiation in the evapotranspiration process and release water vapour that contributes to cool the air in their vicinity. In contrast, built surfaces are composed of a high percentage of non-reflective and water-resistant construction materials. As consequence, they tend to absorb a significant proportion of the incident radiation, which is released as heat, have been recognized as additional causes of the UHI effect.

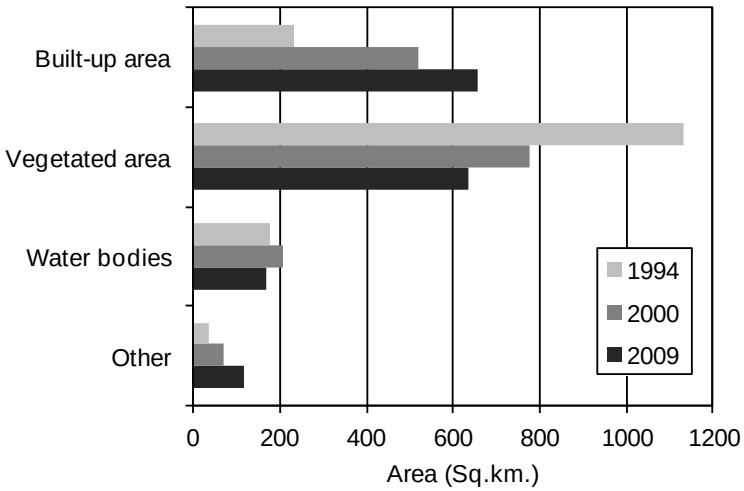

Fig.2. Changes in LULC composition from 1994 **to** 2009

Table.1 Land use/cover statistics (area in sq.km, percentage of the total study area) in BMA from 1994, 2000 and 2009

LULC Types	Year			Changes		
	1994	2000	2009	1994-2000	2000-2009	1994-2009
Built-up area	233.33 (14.80%)	519.87 (32.98%)	657.29 (41.70%)	286.54 (18.18%)	137.43 (8.72%)	423.96 (26.90%)
Vegetated area	1,131.08 (71.76%)	777.52 (49.33%)	636.01 (40.35%)	-353.57 (-22.43%)	-141.51 (-8.98)	-495.07 (-31.41%)
Water bodies	177.69 (11.27%)	207.36 (13.16%)	167.95 (10.66%)	29.67 (1.88%)	-39.40 (-2.50%)	-9.73 (-0.62%)
Other (bare land)	34.00 (2.16%)	71.36 (4.53%)	114.84 (7.29%)	37.36 (2.37%)	43.48 (2.76%)	80.84 (5.13%)

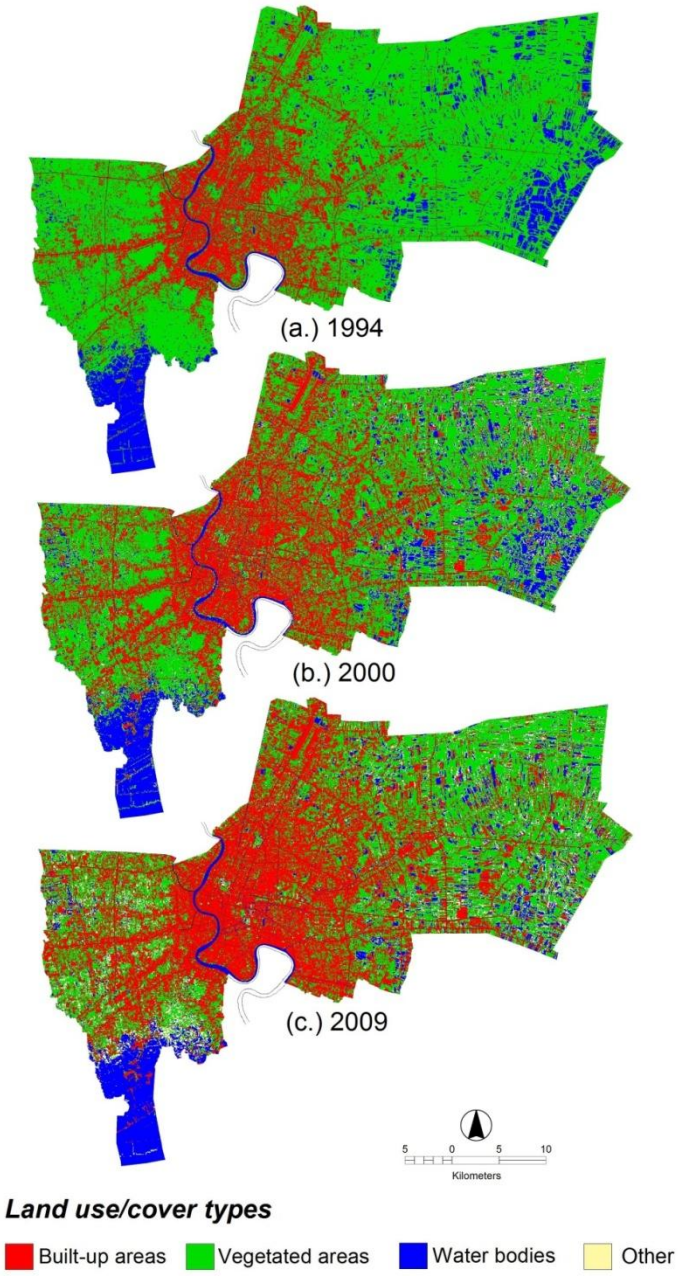

Figs.3. **Land use/cover change in the study area from** 1994 **to** 2009

4.2 The impact of land use/cover changes on LST

The digital remote sensing method provides not only a measure of the magnitude of surface temperatures of the entire metropolitan area, but also the spatial extent of the surface heat island effects. In this study, we selected three Landsat images, i.e., the Landsat 5 TM images on Mar. 5, 1994 (the early summer), Feb. 18, 2000 (the late winter) and Apr. 25, 2009 (the summer), respectively. It was found that average surface temperature (Mean ± S.D.) in the BMA was about 26.01 ± 5.89˚C degree in 1994, but this difference jumped to 37.76 ± 2.84˚C in 2000 and further to 39.79 ± 2.91˚C in 2009, respectively. Figs. 4 show the increasing extent of LST over the study period. In 1994, the areas with higher surface radiant temperature were mainly located in the central urban area and the major district such as; Don Mueang airport district, Khlong Toei port district, also known as Bangkok Port was Thailand's major port for sea transportation of cargo, with a typical strip shaped associated with the traffic road systems. Within the urban central area, numerous sub-centers of LST with higher surface radiant temperature were mainly located in the old and recently developed downtowns at middle section of the Chao Phraya River.

The intensity of urban heat island was defined as the difference between average temperature of UHI area and that of rural area. The intensities of UHI for three dates were listed in Table 1. General patterns of UHI with a maximum LST difference of 8.16 ˚C between urban and rural areas in 1994, the difference jumped to 10.89 ˚C in 2000 and further to 11.50 ˚C in 2009 and the changes were 2.76 ˚C and 0.61 ˚C for 1994–2000 and 2000–2009, respectively (Table 2).

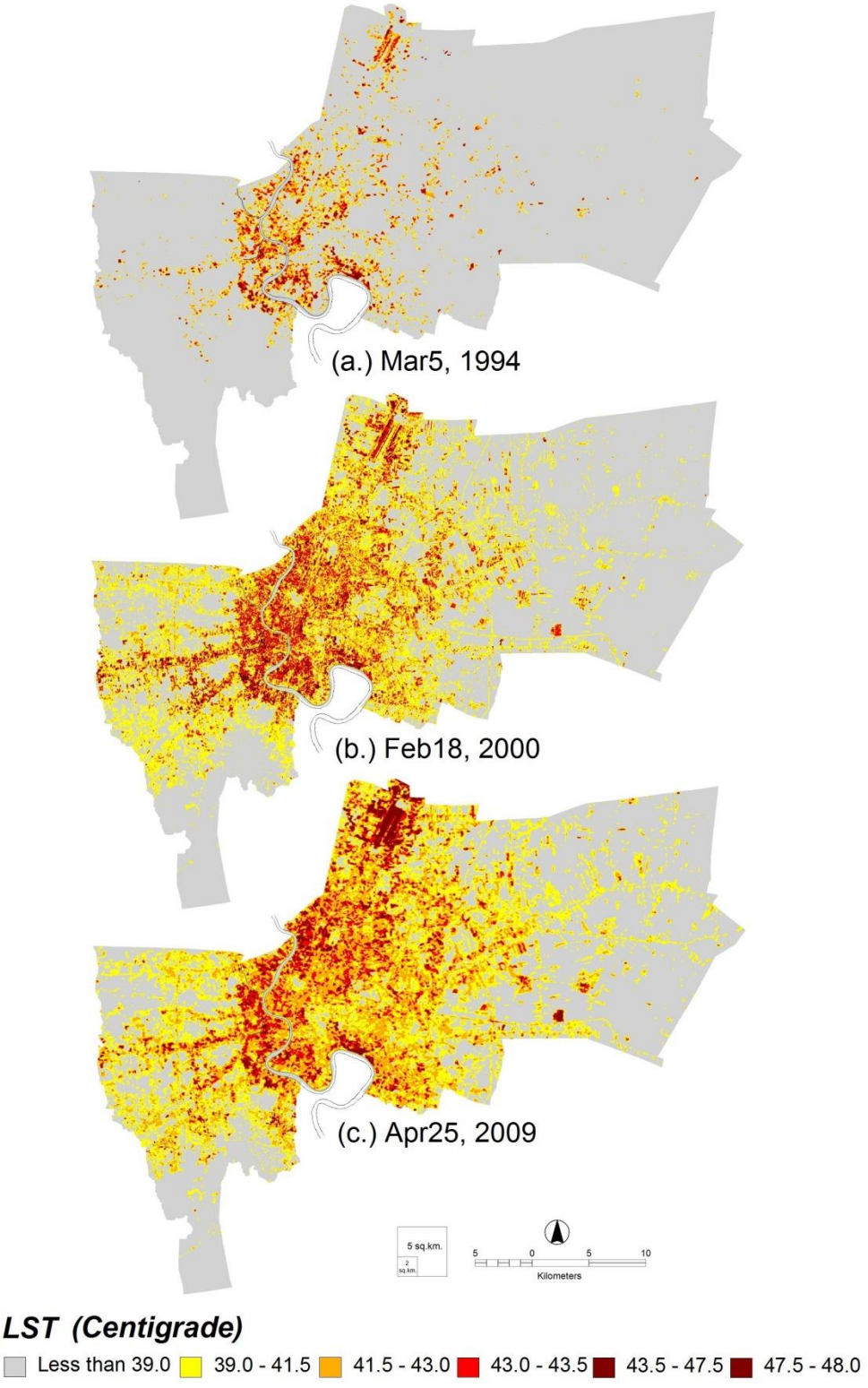

Figs.4. LST derived from Landsat TM (a,b,c) imagery for three different dates

Table.2: Descriptive statistics and intensity of urban heat island of study area for observed years

Statistics	LST_{1994}	LST_{2000}	LST_{2009}
Intensity of SUHI (˚C)	8.16	10.89	11.50
Mean (˚C)	26.01	37.76	39.79
Standard deviation (S.D.)	5.89	2.84	2.91

Quantitatively, Table 3 shows the average LST and NDVI (mean ± S.D.) of each land use/cover type. Clearly, on two dates the built-up area that includes commercial, industrial and residential land exhibited the highest land surface temperature, followed by bare land. The vegetated area and water took third and fourth places, respectively. In comparison to the lower LST of each land cover type in 1994, increasing LST of each land cover type in 2000 and 2009 were detected; indicating seasonal variation should not be neglected when exploring the spatial and temporal pattern of UHI indicated by LST. However, differences in land surface temperatures reflected the impacts of land use changes on the thermal environment. Given the growing extent and magnitude of UHI on three dates, dramatic land use and cover changes in urban fringes and the major satellite towns exacerbated the regional UHI effect.

4.2 The impact of land use/cover changes on greenness

NDVI has been widely used as an indicator of vegetation abundance to estimate LST in studies of urban heat islands (Carson et al., 1994; Gillies and Carlson, 1995; Weng et al., 2004). In this study, NDVI and LST were found to be closely correlated in several LULC categories, especially in vegetated areas (Table 3). Generally, urban areas exhibit smaller NDVI values than non-urban areas, with consistent decrease in the mean NDVI as the mean LST increases. Indeed there is a consistent decline in NDVI with increase level of urban development. NDVI maps for the three dates are shown in Figs. 3. From 1994 to 2009, it was found that average NDVI (mean $\pm$ S.D.) in the BMA was about 0.304 ± 0.353 in 1994 (the early summer), but this difference decreased to 0.146 $\pm$ 0.253 in 2000 (the late winter) and further to 0.016 ± 0.200 in 2009 (the summer), respectively. This explains the fact that there was less vegetation cover interspersed within the developed areas in 2009 in comparison to 2000 and 1994, because vegetation landscapes in urban areas are interspersed with the variegated developed urban structures.

A sample with 6,620 randomly generated points was used to investigate the relationships of LST to NDVI for various LULC types. This explains the pattern between LST and NDVI in the scatter plots of Figs. 8; it appears there are at least two different areas, are not straightforward: When NDVI <-0.5 for March 1994, <-0.35 for February 2000 and <-0.2 for Aprils 2009 imagery, respectively (the relationships between the mean LST and mean NDVI graphed in Fig. 9), which represents heterogeneous effects from diverse non-vegetated areas of urban surfaces, non-vegetated wetland, and bare soil, no stable trend can be identified. In contrast, at higher NDVI values there is an inverse linear association with some variations at the highest NDVI levels on all three graphs, indicating there is a negative correlation between NDVI and LST from late winter to summer. However, the relationship tends to break down in the rural surroundings outside of Bangkok. In comparison to the other three period maps of NDVI (Figs.4 and 5) look very different with no evident association between the LST and the NDVI, which further implies using NDVI to understand LST is complicated since NDVI itself suffers strong seasonal changes.

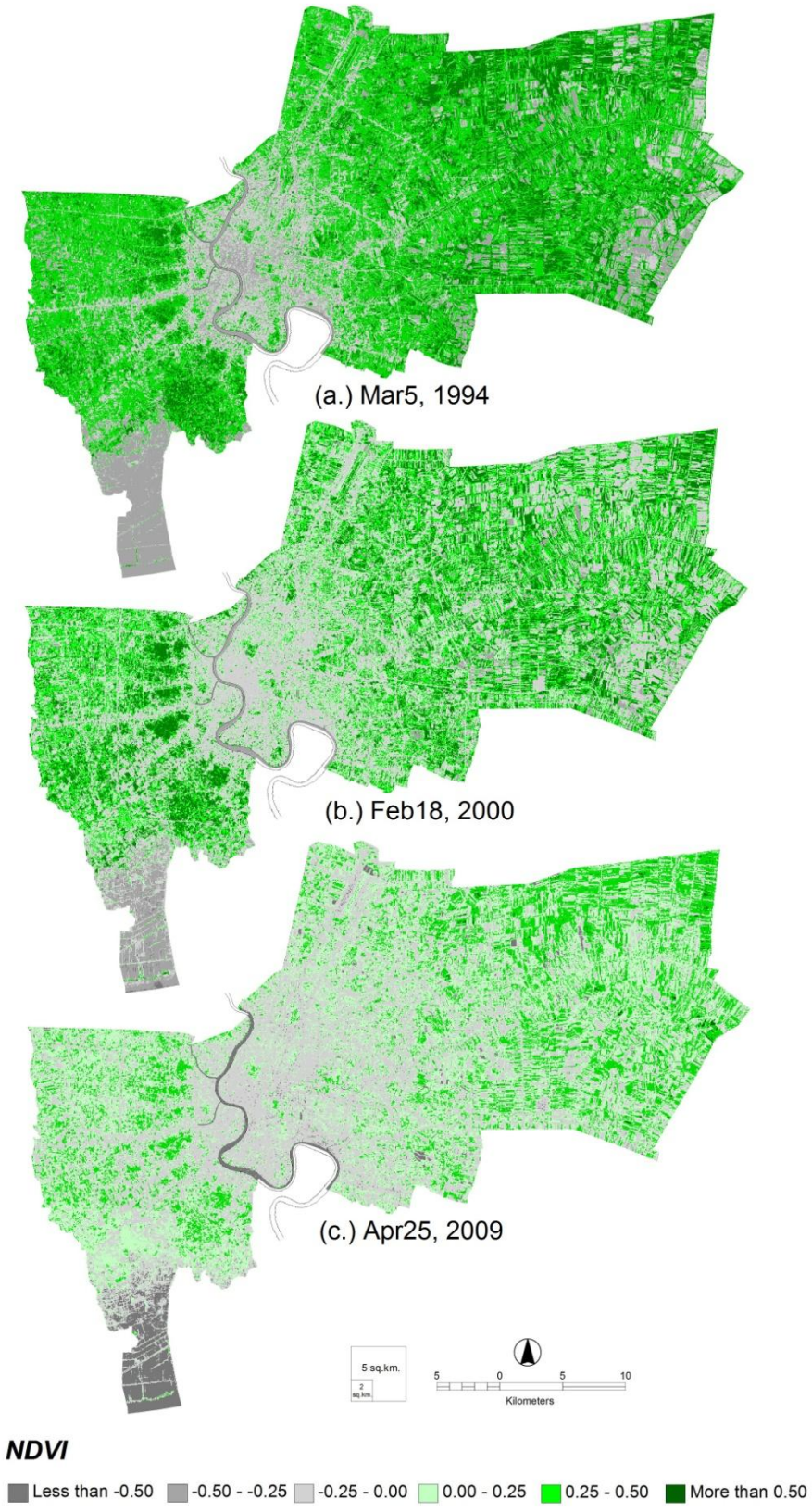

Figs.5. NDVI derived from Landsat TM (a,b,c) imagery for three different dates

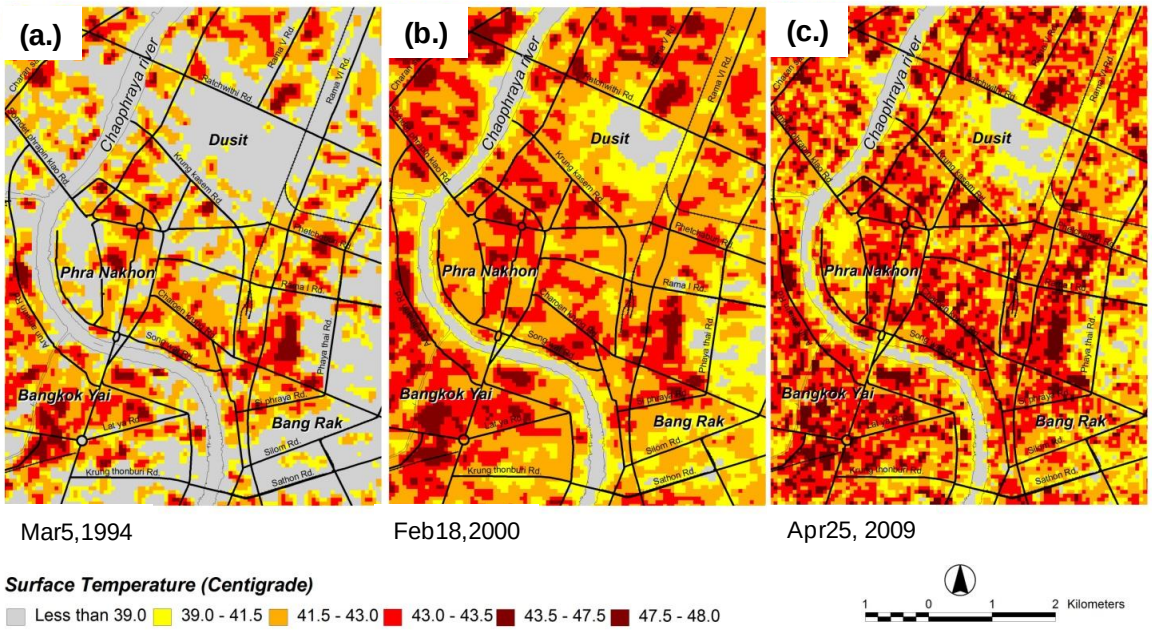

Figs.6. Spatial distribution patterns of LST in the Rattanakosin Island from the TM images acquired on (a.) 1994, (b.) 2000, and (c.) 2009

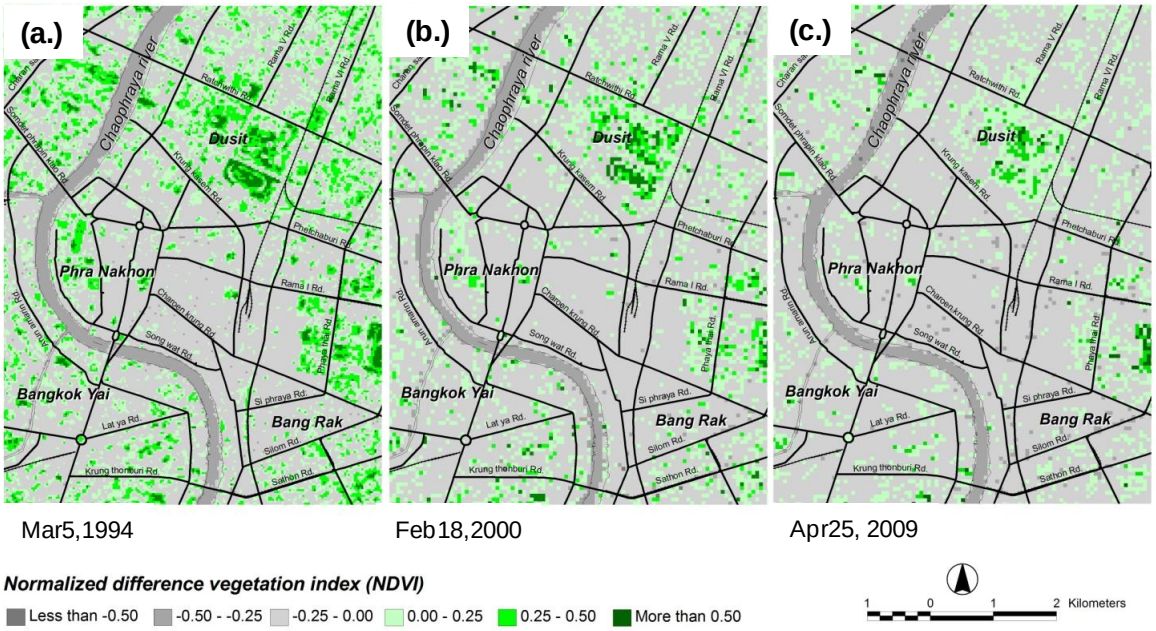

Figs.7. Spatial distribution patterns of NDVI in the Rattanakosin Island the TM images acquired on (a.) 1994, (b.) 2000, and (c.) 2009

Table.3: Average LST (˚C) and NDVI (mean ± S.D.) for various land uses/cover types

LULC Types	1994		2000		2009	
	LST	NDVI	LST	NDVI	LST	NDVI
Built-up area	35.68±5.32	-0.137±0.099	40.04±1.79	-0.283±0.105	41.51±1.64	-0.497±0.182
Vegetated area	25.04±3.15	0.213±0.227	37.76±1.38	0.149±0.132	39.74±1.40	0.016±0.171
Water bodies	22.48±2.53	-0.863±0.206	36.74±1.01	-0.556±0.218	38.18±0.94	-0.368±0.208
Other	26.78±4.81	-0.691±0.192	37.06±1.21	-0.114±0.238	39.03±0.92	0.103±0.076

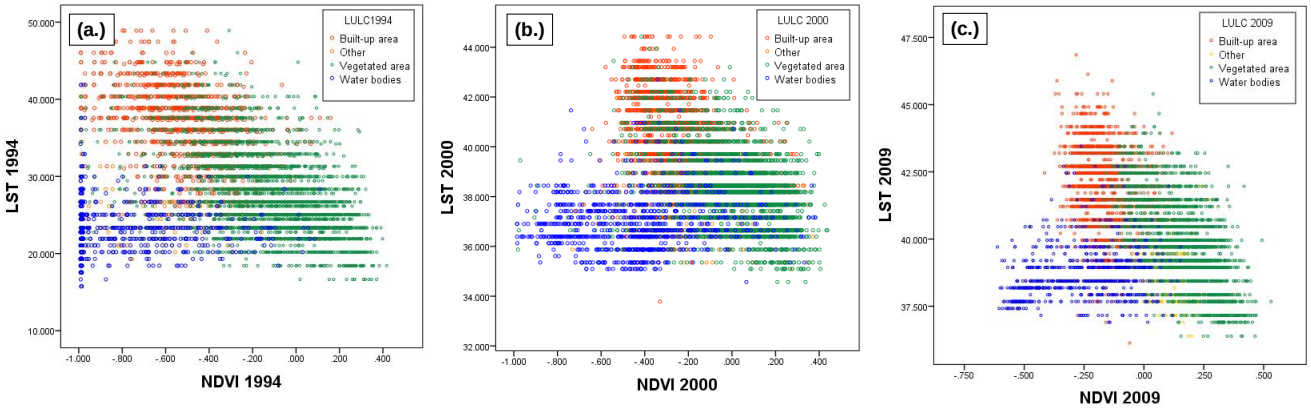

Figs.8. Scatterplots of LST versus NDVI for various LULC types of three different dates (a.) 1994, (b.) 2000, and (c.) 2009

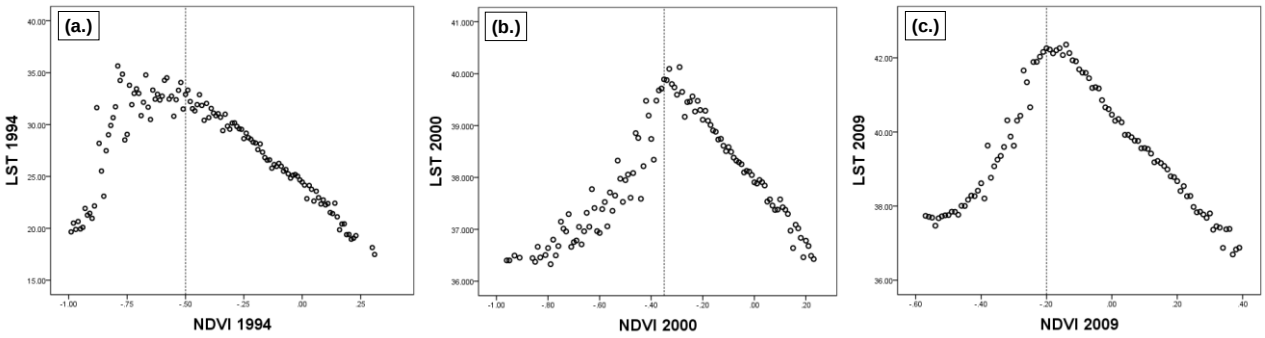

Figs.9. Relationship of mean LST versus mean NDVI (a.) 1994, (b.) 2000, and (c.) 2009

Table.4: Pearson's correlation coefficients between LST and NDVI for various land uses/cover types

LULC Types	1994	2000	2009
Built-up area	-0.414*	-0.391*	-0.343*
Vegetated area	-0.311*	-0.498*	-0.556*
Water bodies	-0.012*	-0.019*	-0.032*
Other (bare land)	-0.054*	-0.033*	-0.041*

**Significant at P=0.05*

Pearson's correlation coefficient of LST in 1994 to 2009, were negatively correlated with NDVI for all LULC categories in third years (Table.4). This significant negative correlation between LST and NDVI implied that the higher biomass a land cover had, the lower its LST was. This relationship has determined that due to the associated changes in NDVI, changes in LULC would have an indirect impact on LST.

5. CONCLUSIONS

This study has examined LULC changes in Bangkok metropolitan area, Thailand, from 1994 to 2009. The results indicate that urban/built-up areas expanded dramatically, while agricultural land declined. This decrease was also evident between 1994 and 2000, when vegetated area was further shrunk about 22% of the total area, was converted to other land use. The observed changes in LULC were largely attributed to population pressure on the land, a rapidly growing economy, poor land use planning, and the inconsistency in the governmental policies. Changes in LULC were accompanied by changes in LST. From 1994 to 2000, the urban or built-up surface temperature climbed, and continued to increase in BMA between 2000 and 2009. Moreover, temperature differences between the urban/built-up and the surrounding rural areas significantly widened. This could lead to an intensified urban heat island effect in the urban areas. The abundance of vegetation was an important factor influencing LST. This demonstrated that the decrease of biomass primarily triggered the impacts of urban expansion on LST. The application of remote sensing and GIS proved to be an efficient way to detect LULC and to evaluate its effect on LST. This made it possible to investigate the impacts of human activities on the environment as done in this study. In future studies, there is the need to focus on: *(i)* evaluation of the impact of the urban morphology on urban climate, and *(ii)* explore the relationship between urban planning (For example, green cover ratio and floor area ratio) indicators and climate indicators.

Acknowledments

The authors would like to express their sincere thanks to the anonymous reviewers for their constructive suggestions, comments, and helps. This research is supported by the Department of Civil Engineering and Architecture, Graduate School of Science and Engineering, Saga University, Japan and Geo-Informatics and Space Technology Development Agency (Public Organization): GISTDA, Thailand.

References

Akbari,H.,Rosenfeld,A.,Taha,H.,&Gartland,L.(1996). Mitigation of summer urban heat islands to save electricity and smog. *In 76th Annual American Meteorological Society Meeting Atlanta*, GA.

Akbari, H.,Pomerantz,M.,&Taha,H.(2001). Cool surfaces and shade trees to reduce energy use and improve air quality in urban areas. *Solar Energy*, 70, 295–310.

Boonjawat, J., Niitsu, K., Kubo, S., 2000. Urban heat island: thermal pollution and climate change in Bangkok. *Report of the Southeast Asia START Regional Center*, www address, http://www.start.or.th/heatisland/.

Barsi, J.A., J.R. Schott, F.D. Palluconi, D.L. Helder, S.J. Hook, B.L. Markham, G. Chander, E.M. O'Donnell, (2003). Landsat TM and ETM+ thermal band calibration. *Canadian Journal of Remote Sensing*, 29(2), 141-153.

Chen, Yunhao,Wang, Jie, & Li, Xiaobin (2002). A study on urban thermal field in summer based on satellite remote sensing. *Remote Sensing for Land and Resources*, 4, 55−59.

Chen, Z. M., Babiker, I. S., Chen, Z. X, Komaki, K., Mohamed, M. A. A., & Kato, K. (2004). Estimation of interannual variation in productivity of global vegetation using NDVI data. *International Journal of Remote Sensing*, 25 (16), 3139−3150.

Chen, X.L., Zhao, M.Z., Li, P.X., Yin, Z.Y., (2006). Remote sensing image-based analysis of the relationship between urban heat island and land use/cover changes. *Remote Sensing of Environment*, 104, 133-146.

Chen, D., and W. Brutsaert (1998), Satellite-sensed distribution and spatial patterns of vegetation parameters over a tallgrass prairie, J. *Atmos. Sci.*, 55(7), 1225-1238.

Chander, G., Markham, B., (2003). Revised Landsat-5 TM radiometric calibration procedures and post-calibration dynamic ranges. *IEEE Transactions on Geoscience and Remote Sensing*, 41 (11), 2674-2677.

Carson, T. N., Gillies, R. R., and Perry, E. M. (1994). A method to make use of thermal infrared temperature and NDVI measurements to infer surface soil water content and fractional vegetation cover. *Remote Sensing Reviews*, 9, 161-173.

Gallo, K. P., Tarpley, J. D., McNab, A. L., & Karl, T. R. (1995). Assessment of urban heat islands: A satellite perspective. *Atmospheric Research*, 37, 37−43.

Gallo, K. P., & Owen, T. W. (1998a). Assessment of urban heat island: A multisensory perspective for the Dallas-Ft. Worth, USA region. *Geocarto International*, 13, 35−41.

Gallo, K. P., & Owen, T. W. (1998b). Satellite-based adjustments for the urban heat island temperature bias. *Journal of Applied Meteorology*, 38, 806−813.

Gillies, R. R., Carlson, T. N., Cui, J., Kustas, W. P. and Humes, K. S., (1997). A verification of the 'triangle' method for obtaining surface soil water content and energy fluxes from remote measurement of the Normalized Difference Vegetation Index (NDVI) and surface radiant temperature. *International Journal of Remote Sensing,* 18 , 3145-3166.

Gillies, R. R., and Carlson, T. N. (1995) .Thermal remote sensing of surface soil water content with partial vegetation cover for incorporation into climate models. *Journal of Applied Meteorology*, 34, 745-756.

Hawkins, T. W., Brazel, A. J., Stefanov, W. L., Bigler, W., & Saffell, E. M. (2004). The role of rural variability in urban heat island determination for Phoenix, Arizona. *Journal of Applied Meteorology*, 43, 476−486.

Kalnay and Cai, (2003), Impact of urbanization and land-use change on climate, *Nature*, 423(29), 528–531.

Kiattiporn W., Somchai M., Nipon K.,&Wattanapong R. (2008). The impacts of climatic and economic factors on residential electricity consumption of Bangkok Metropolis. *Energy and Buildings*, 40, 1419-1425.

Landsberg, (1981), The urban climate, Academic Press, New York (1981).

Myneni, R. B., Dong, J., Tucker, C. J. Kaufmann, R. K. Kauppi, P. E., Liski, J., Zhou, L., Alexeyev, V., & Hughes,M. K., (2001). A large carbon sink in the woody biomass of Northern forests. *Proc. Natl. Acad. Sci. U.S.A.*, 98, 14784-14789.

Owen, T. W., Carlson, T. N., & Gillies, R. R. (1998). An assessment of satellite remotely-sensed land cover parameters in quantitatively describing the climatic effect of urbanization. *International Journal of Remote Sensing*, 19, 1663−1681.

Purevdorj, T. S., Tateishi, R., Ishiyama, T., & Honda, Y. (1998). Relationships between percent vegetation cover and vegetation indices. *International Journal of Remote Sensing*, 19(18), 3519−3535.

Poumadere, M.,Mays,C.,LeMer,S.,&Blong,R.(2005).The 2003heat wave in France: Dangerous climate change here and now. *Risk Annual*, 25(6), 1483–1494.

Rao, P. K. (1972). Remote sensing of urban "heat islands" from an environmental satellite. *Bulletin of the American Meteorological Society*, 53, 647−648.

Streutker, D. R. (2002). A remote sensing study of the urban heat island of Houston, Texas. *International Journal of Remote Sensing*, 23(13), 2595−2608.

Schmidt, H., Karnieli, A., (2000). Remote sensing of the seasonal variability of vegetation in a semi-arid environment. *Journal of Arid Environments*, 45 (1), 43-60.

Schroeder et al., (2006). Radiometric correction of multi-temporal Landsat data for characterization of early successional forest patterns in western Oregon, *Remote Sensing of Environment*, 103, 16–26.

Tian, Qingjiu, & Xiangjun, Min (1998). Advances in study on vegetation indices. *Advance in Earth Sciences*, 13(4), 327−333.

Voogt, J. A., & Oke, T. R. (2003). Thermal remote sensing of urban areas. *Remote Sensing of Environment*, 86, 370-384.

Weng, Q., Lu, D., and Schubring, J. (2004). Estimation of land surface temperature – vegetation abundances relationship for urban heat island studies. *Remote Sensing of Environment*, 89, 467-483.

Wang, J., Rich, P. M., Price, K. P., & Kettle, W. D. (2004). Relations between NDVI and tree productivity in the central Great Plains. *International Journal of Remote Sensing*, 25(16), 3127−3138.

White,M.A.,Nemani,R.R.,Thornton,P.E.,&Running,S.W. (2002).Satellite evidence of phonological differences between urbanized and rural areas of the eastern United States deciduous broadleaf forest. *Ecosystems*, 5, 260–277.

Weng, Q., Lo, C.P., (2001). Spatial analysis of urban growth impacts on vegetative greenness with Landsat TM data. *Geocarto International*, 16 (4), 17–25.

Weng, Q. (2001). A remote sensing-GIS evaluation of urban expansion and its impact on surface temperature in Zhujiang Delta, China. *International Journal of Remote Sensing*, 22(10), 1999−2014.

Yuan, F., Sawaya, K. E., Loeffelholz, B. C., & Bauer, M. E. (2005). Land cover mapping and change analysis in the Twin Cities Metropolitan Area with Landsat remote sensing. *Remote Sensing of Environment*, 98(2.3), 317-328.

View publication stats